

Optically detected magnetic resonance study of antisite-to-acceptor and related recombination processes in as-grown InP:Zn

L. H. Robins* and P. C. Taylor

Department of Physics, University of Utah, Salt Lake City, Utah 84112

T. A. Kennedy

Naval Research Laboratory, Washington, D.C. 20375-5000

(Received 7 June 1988)

The paramagnetic state of the phosphorus-on-indium antisite (P_{In}) has been observed by optically detected magnetic resonance (ODMR) in as-grown zinc-doped indium phosphide (zinc concentration $\approx 10^{16} \text{ cm}^{-3}$). The antisite resonance is seen both as enhancing the antisite-to-acceptor photoluminescence (PL) at 0.8 eV and as quenching the shallow-donor to acceptor PL at 1.37 eV. The g value ($g = 2.006$) and hyperfine constant ($A = 0.100 \text{ cm}^{-1}$) are in good agreement with previous results on electron-irradiated p -type InP. The dependence of the ODMR on microwave power, microwave modulation frequency, and photoexcitation intensity is examined, and a rate-equation model is developed for the important recombination processes. The experimental results suggest that the antisite-to-acceptor recombination rate is approximately $4 \times 10^4 \text{ s}^{-1}$; the antisite electron spins are unthermalized, but recombine with spin-thermalized holes; and the antisite concentration may be greater than $2 \times 10^{15} \text{ cm}^{-3}$. Two other resonances are also observed, a shallow donor resonance ($g = 1.217$) and an unidentified broad resonance ($g = 2.0$).

I. INTRODUCTION

The P_{In} antisite in InP was first identified by conventional electron paramagnetic resonance¹ (EPR) in an electron-irradiated liquid-encapsulated Czochralski grown single crystal, and subsequently by two different optically detected magnetic resonance²⁻⁴ (ODMR) techniques. ODMR has been one of the most useful probes of the atomic and electronic structure of antisites and other intrinsic defects in semiconductors, for the following reasons. While conventional EPR is restricted to stable or metastable paramagnetic states, optically detected magnetic resonance (ODMR) can be applied to defects with short-lived paramagnetic excited states and nonmagnetic ground states. In addition, while conventional EPR generally requires more than $10^{15} \text{ spins/cm}^3$ in order to observe a resonance, even in bulk samples, ODMR is potentially sensitive to a much smaller concentration of defects. In magnetic-circular-dichroism ODMR (MCD ODMR), magnetic resonance in a defect ground state is detected as a change in the optical absorption of circularly polarized light.^{2,3} In photoluminescence ODMR (PL ODMR), magnetic resonance in an excited state is detected as a change in the intensity or polarization of the recombination radiation.⁴

More recently, the resonance of the antisite in non-irradiated zinc-doped LEC-grown InP (Ref. 5) was observed by PL ODMR, and, in addition, a new antisite-defect complex was identified by the same technique in phosphorus-annealed InP.⁶ In all of the above PL ODMR studies, the antisite resonance was observed as enhancing a deep PL band at 0.8–0.9 eV. (The antisite-related PL appears to dominate the total deep-level PL emission spectrum in heavily electron-irradiated InP, but

is only seen as a small shoulder on top of other deep-level PL bands in the as-grown samples^{4,5}.)

New PL ODMR results are presented in the present study. We show that the antisite resonance in as-grown InP:Zn can be observed both as an enhancing resonance of the deep-level PL at 0.8 eV and as a quenching resonance, of approximately equal magnitude, of the shallow-donor to acceptor PL at 1.37 eV. Other ODMR signals are also detected at 1.37 eV. The dependence of the ODMR on photoexcitation intensity, microwave power, and microwave modulation frequency is discussed. We develop a simple rate-equation model for the antisite-to-acceptor and competing shallow-donor to acceptor recombination that is consistent with the results and provides an estimate of the concentration of antisite defects.

II. EXPERIMENTAL PROCEDURE

The InP sample used in the present study was a Zn-doped LEC-grown single crystal with a hole density of $\sim 10^{16} \text{ cm}^{-3}$ (NRL sample 2-74-H, grown by R.L. Henry). The experiments were performed in a 16-GHz ODMR spectrometer. The microwave cavity of this spectrometer was placed in the sample chamber of a liquid-helium cryostat containing a superconducting magnet; all measurements were performed with the sample and microwave cavity immersed in superfluid He at $T = 2 \text{ K}$. The PL was excited by an Ar^+ laser at 2.41 or 2.54 eV, or by a He-Ne laser at 1.96 eV. The deep-level PL at 0.8 eV was detected by a liquid-nitrogen-cooled germanium photodiode with a 1.1-eV long-pass or a 0.8-eV band-pass filter. The shallow-donor to acceptor PL at 1.37 eV was detected by a silicon photodiode with a 1.5-

eV long-pass or a 1.35-eV band-pass filter. The PL was collected in the direction parallel to the magnetic field. The circular polarization of the emitted light could then be analyzed by a Fresnel rhomb (a prism that produces a quarter-wave phase shift in the polarization) and infrared linear polarizer. The microwave power was square-wave modulated at frequencies from 10 Hz to 100 kHz, with a modulation depth close to 100%, by a *p-i-n* diode switch. Phase-sensitive detection was used to measure the change in PL intensity at the microwave modulation frequency.

III. RESULTS

ODMR spectra obtained by monitoring the P_{In} -antisite-related PL at 0.8 eV and the shallow-donor to acceptor PL at 1.37 eV are shown in Figs. 1(a) and 1(b), respectively. For conciseness, the antisite resonance detected at 0.8 eV will be denoted the antisite-antisite (AS-AS) resonance, and the antisite resonance detected at 1.37 eV will be denoted the antisite-donor-acceptor (AS-DA) resonance. The AS-DA resonance is observed with better

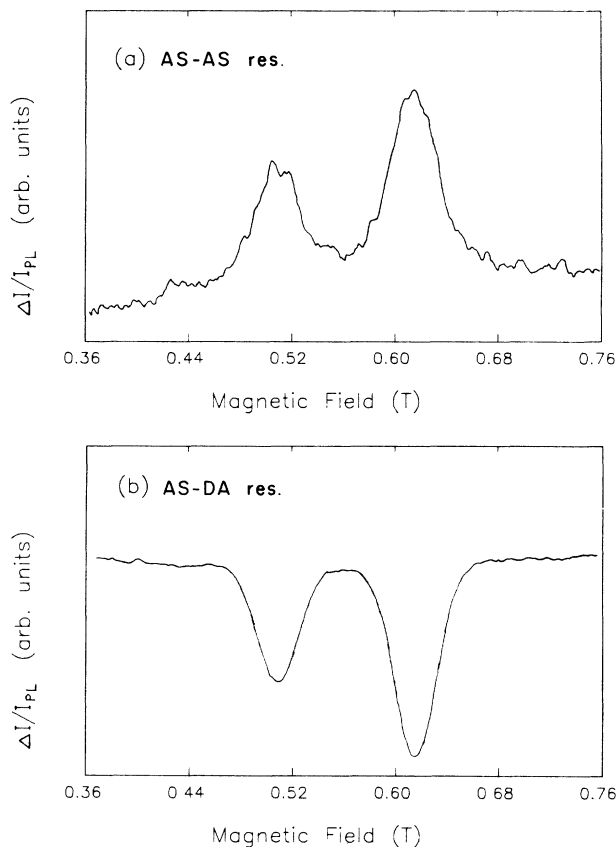


FIG. 1. (a) Spectrum of the antisite ODMR enhancing the antisite to acceptor PL at 0.8 eV. Spectrum shown here was obtained by averaging many individual spectra, with photoexcitation intensity, 1 W/cm²; microwave resonance frequency, 15.9 GHz; microwave power, 20 mW; variable modulation frequency. (b) Spectrum of the antisite ODMR quenching the shallow-donor to acceptor PL at 1.37 eV, obtained by averaging many individual spectra; other experimental parameters same as for (a).

signal-to-noise than the AS-AS resonance because of the differences in PL intensity and detector sensitivity at the two photon energies, but the peak positions and linewidths of the two are equal within experimental uncertainty.

The P_{In} antisite resonance is split into two lines because of the strong hyperfine interaction between the electron spin and the central ³¹P ($I = \frac{1}{2}$) nucleus. Unresolved ligand hyperfine interactions give rise to the large linewidth (0.039 T) of each component. [In a recent study of the antisite by optically detected electron-nuclear double resonance, hyperfine interactions with the first and second ligand shells⁷ were resolved. The first shell was shown to consist of four tetrahedrally coordinated phosphorus atoms, and the second shell was shown to consist of 12 indium atoms, confirming that the antisite generally occurs as an isolated defect rather than as part of a defect complex.] The spin Hamiltonian parameters, g and A , can be obtained from the peak positions of the two hyperfine-split lines, 0.5079 and 0.6148 T. The values of the parameters thus obtained, taking into consideration both the first- and second-order hyperfine interaction terms, are $g = 2.006 \pm 0.005$ and $A = 0.100 \pm 0.002$ cm⁻¹, in excellent agreement with the values obtained previously by the MCD ODMR technique.^{3,8}

In addition to the resonances shown in Fig. 1, a large background microwave modulation of the PL intensity, almost independent of magnetic field, was observed. The magnitude of the background varied with the experimental conditions, in particular microwave power and photoexcitation intensity, but was generally more than twice as large as the ODMR at 0.8 eV and more than ten times the ODMR at 1.37 eV. Similar effects are often seen in ODMR of semiconductors and may arise either from microwave heating or from microwave ionization of impurity levels.⁹

The ODMR spectrum detected at 1.37 eV has a complicated dependence on photoexcitation intensity. When the intensity is reduced by a factor of 50, from 3×10^{18} photons/cm² sec (the level of Fig. 1) to 5×10^{16} photons/cm² sec, a broad peak with $g = 2.0$ becomes apparent in addition to the antisite resonance. The ODMR spectrum at the lower photoexcitation level is shown in Fig. 2. The excitation intensity dependence of the magnitude of the ODMR, for both the antisite and the broad $g = 2$ resonance, is plotted in Fig. 3. The magnitude of the antisite ODMR first decreases and then increases with excitation intensity, while the $g = 2$ resonance decreases monotonically; at high intensity, the latter cannot be distinguished from the wings of the two antisite resonance lines (compare Figs. 1 and 2).

Still another resonance detected as a quenching of the 1.37-eV PL is shown in Fig. 4. The low g value of 1.217 ± 0.003 identifies this as a resonance of electrons either bound to shallow donors or in the conduction band. (Values previously obtained for the electron g value in InP are 1.26 ± 0.05 , by spin-polarized conduction electron spin resonance,¹⁰ and 1.22 ± 0.03 , by ODMR of the deep acceptor PL band¹¹ in InP:Mn.)

The saturation behavior of the antisite ODMR was examined. The microwave power dependence of the magni-

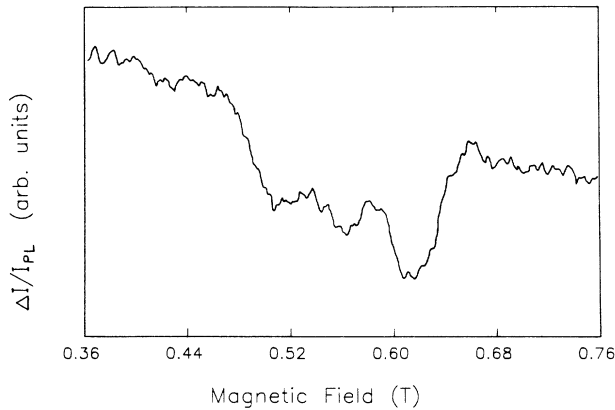


FIG. 2. Spectrum of the ODMR quenching the shallow-donor to acceptor PL; photoexcitation intensity reduced to 10 mW/cm². Microwave frequency is 15.9 GHz, microwave power is 20 mW, modulation frequency is 500 Hz.

tudes of the AS-AS and AS-DA resonances, for power levels from 0.6 to 200 mW, is shown in Fig. 5. The similarity between the power dependences of the two resonances suggests that both arise from the same set of states. The magnitudes vary approximately as the square root of the microwave power over most of the range. This behavior is as expected for an inhomogeneously broadened resonance line when the power is high enough to saturate the individual spin packets but not high enough to saturate the entire inhomogeneous distribution.

The magnitude of the antisite ODMR also depends on the frequency of the modulation of the microwave power. Both the in-phase and quadrature components of the ODMR, relative to the phase of the microwave power modulation, are shown in Fig. 6. Care was taken in this experiment to ensure that the photodetection system response time was faster than the modulation frequency. The ODMR decreases rapidly with increasing modulation frequency f for $f > 1$ kHz, as shown for the AS-AS

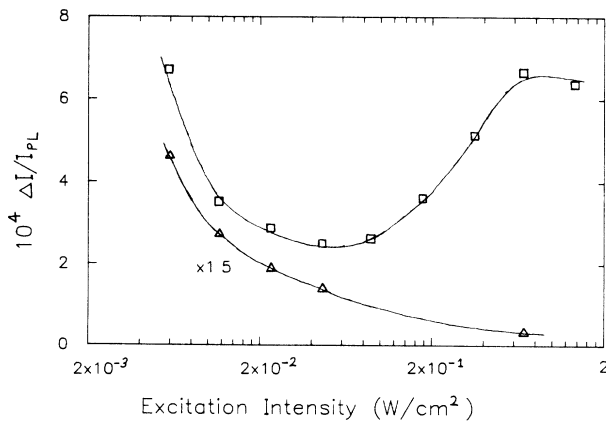


FIG. 3. Photoexcitation intensity dependence of antisite resonance (\square) and broad $g=2$ resonance (\triangle) of shallow-donor to acceptor PL. Microwave frequency is 15.9 GHz, microwave power is 20 mW, modulation frequency is 500 Hz. Full curves are drawn to guide the eye.

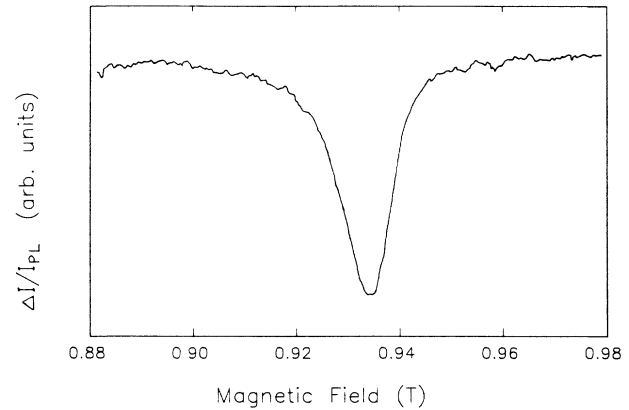


FIG. 4. Spectrum of the shallow donor or conduction electron ODMR, also observed to quench the shallow-donor to acceptor PL. Photoexcitation intensity is 1 W/cm², microwave frequency is 15.91 GHz, microwave power is 20 mW, modulation frequency is 500 Hz. Note that this spectrum is observed at higher magnetic field than the others.

resonance in Fig. 6(a). The frequency dependence of the AS-DA resonance, shown in Fig. 6(b), is similar, but the high-frequency roll-off is shifted to slightly lower frequency for the latter resonance. The in-phase component approaches a maximum and the quadrature component vanishes for both resonances at low frequency, $f < 200$ Hz. The solid lines shown in Fig. 6 are a fit to the data derived from the rate-equation model described in the Appendix.

The AS-DA ODMR spectrum at low photoexcitation intensity was measured at a modulation frequency $f = 50$ Hz, in addition to the measurement at $f = 500$ Hz shown in Fig. 2. The ODMR signal was found to decrease with increasing frequency, from $f = 50$ Hz to 500 Hz, slightly more at the lower excitation level than at the high excitation level of Fig. 6. It appears therefore that the roll-off of the ODMR signal as a function of modulation frequency begins at lower frequency at the lower photoexcitation level.

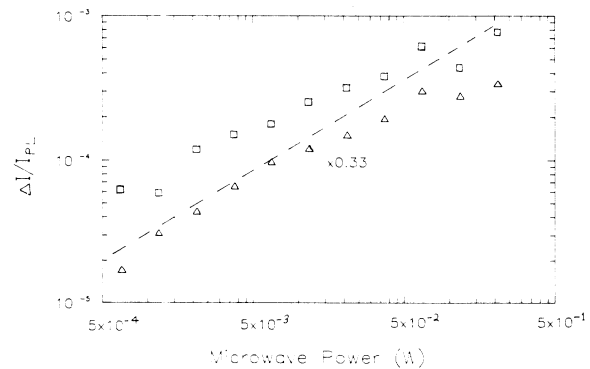


FIG. 5. Microwave power dependence of antisite ODMR, enhancing signal at 0.8 eV (\triangle) and quenching signal at 1.37 eV (\square). Photoexcitation intensity is 1 W/cm², microwave frequency is 15.9 GHz, modulation frequency is 500 Hz. Dashed line shows square-root dependence expected for inhomogeneously broadened resonance line shape.

The magnitude of the ODMR is expressed as the fractional change in PL intensity on resonance $\Delta I/I_0$. The maximum value of $\Delta I/I_0$ for the antisite resonances at 16 GHz can be estimated from the results presented in Figs. 2, 5, and 6. In the limit of low-frequency modulation, at a microwave power level of 20 mW, the values obtained by summing the two hyperfine-split peaks are 6×10^{-4} for the AS-AS resonance and -8×10^{-4} for the AS-DA resonance (Fig. 6). As seen from the microwave power dependence of Fig. 5, the magnitude of both resonances can be increased by approximately a factor of two at microwave powers higher than 20 mW. Finally, according to the results presented in Fig. 2, $\Delta I/I_0$ is maximum at the high photoexcitation intensity used to obtain the data of Figs. 5 and 6. Thus the maximum value of $\Delta I/I_0$, under conditions of low-frequency modulation, high microwave power, and high photoexcitation intensity, is 1.2×10^{-3} for the AS-AS resonance and -1.6×10^{-3} for the AS-DA resonance.

The magnitude of the high-field peak in the hyperfine-

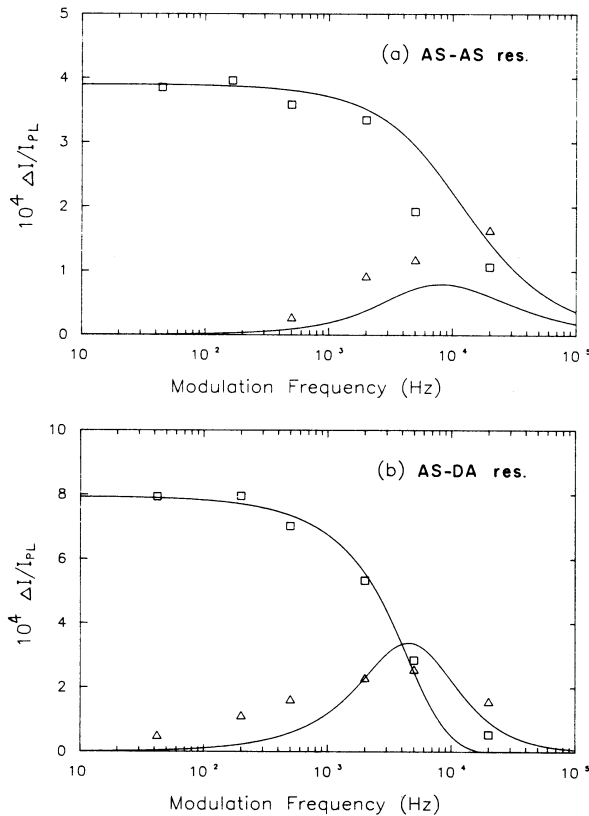


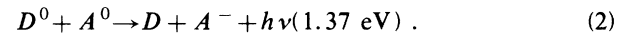
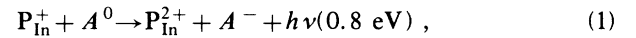
FIG. 6. (a) Modulation frequency dependence of antisite ODMR, enhancing signal at 0.8 eV. In-phase (\square) and quadrature (\triangle) components of response shown. Photoexcitation intensity is 1 W/cm^2 , microwave frequency is 15.9 GHz, microwave power is 20 mW. Solid line is fit to rate-equation model described in Appendix with $R = 4 \times 10^4 \text{ s}^{-1}$ and $\eta = 0.2$. (b) Modulation frequency dependence of antisite ODMR, quenching signal at 1.37 eV. In-phase (\square) and quadrature (\triangle) components of response shown. Experimental parameters same as for (a). Solid line is fit to rate-equation model with same parameters as (a).

split ODMR spectrum is larger than the magnitude of the low-field peak, as is apparent from Fig. 1. The ratio of the high-field to the low-field peak is approximately 1.47 for the AS-AS resonance and 1.68 for the AS-DA resonance. A small effect due to circular polarization, of the order of 10% of the unpolarized ODMR, was seen for the AS-DA resonance. The AS-AS resonance could not be observed with sufficient signal-to-noise ratio while the polarizing filter was inserted to detect a similar effect.

Photoexcitation energies of 1.96, 2.41, and 2.54 eV were used in these experiments. No dependence of the magnitude or form of the P_{In} antisite ODMR on excitation energy was seen at these values.

IV. DISCUSSION

The observation that the antisite resonance quenches the shallow donor to acceptor PL at 1.37 eV provides support for the model of Deiri *et al.*,⁸ according to which the antisite-related PL at 0.8 eV, at least in *p*-type material, arises from the recombination of an electron bound to an antisite with a hole bound to an acceptor. Antisites and shallow donors may then be competing recombination centers for acceptor-bound holes. The recombination processes may be written as



Here, P_{In}^+ is the paramagnetic state of the antisite, occupied by one electron, and P_{In}^{2+} is the nonmagnetic fully ionized state. Similarly, D^0 is the neutral state of the donor, occupied by one electron, A^0 is the neutral state of the acceptor, occupied by one hole, and D^+ and A^- are the ionized states of the donor and acceptor. An energy-level diagram illustrating the competing recombination processes (1) and (2) is presented in Fig. 7.

It is assumed that the antisites and shallow donors are fully compensated by Zn acceptors; thus all of the donor levels are fully ionized in the ground state (D^+ and P_{In}^{2+}). This assumption is consistent with the observation that

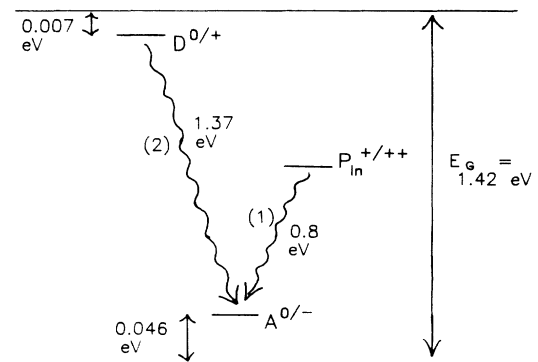


FIG. 7. Energy-level diagram showing the antisite (P_{In}^{2+}), shallow-donor ($D^{0/+}$), and zinc-acceptor [$A^{0/-}$ (Zn)] states in the band gap of InP and the two competing recombination processes: the antisite to acceptor transition (1) and the shallow-donor to acceptor transition (2).

too few antisites are paramagnetic (P_{In}^+) in the ground state to observe by EPR or MCD ODMR. It is also assumed that the doubly occupied state of the antisite (P_{In}^0), if present at all, does not have a significant effect on the recombination processes studied by ODMR. At high photoexcitation intensities, conduction-band to acceptor recombination may become an important process. The band to acceptor PL occurs at slightly higher photon energy than the shallow-donor to acceptor PL (1.378 eV versus 1.373 eV); the two transitions generally give rise to one unresolved peak in the PL spectrum. We will not distinguish further between these two possible hole recombination processes.

The above model for the recombination is easiest to treat quantitatively if it is assumed that each antisite is uniquely paired with one acceptor and can recombine only with that one. Then there is a fixed number of antisite-acceptor pairs, each of which exists in one of four possible charge states at any one time: (P_{In}^+, A^0), (P_{In}^+, A^-), (P_{In}^0, A^+), or (P_{In}^0, A^-); there are six possible states altogether including the spin ($=\frac{1}{2}$) of the P_{In}^+ antisite. An enhancement in the rate of antisite-to-acceptor recombination [Eq. (1)] reduces the number of pairs containing a neutral acceptor, and therefore reduces the number of acceptors available for recombination by the competing process [Eq. (2)]. This model is treated in more detail in the Appendix, and rate equations for the important processes are presented. (A similar model was developed by Verity *et al.*¹² for the ODMR observed in a system where two types of acceptor centers of different depths act as competing radiative recombination centers for the same set of shallow-donor electrons.)

The pair model for donor-acceptor recombination should be valid as long as the average donor-acceptor separation is much larger than the Bohr radius of the more extended wave function, according to the results of Dunstan and Davies.¹³ The Zn acceptor density in the sample is estimated to be 10^{16} cm^{-3} . Because the sample is *p* type, the residual shallow donors must be fully compensated; the density of Zn acceptors must therefore be greater than twice the antisite density (the antisites are double donors) plus the shallow-donor density. Because the acceptors are more numerous than the antisites, the average separation of an antisite-acceptor pair is defined as the average distance from a randomly selected antisite to the nearest neighboring acceptor, and this distance is in turn approximately equal to the average acceptor-acceptor separation of 46 nm (for an acceptor density of 10^{16}). The acceptor wave function is more extended than the antisite wave function;⁷ from the acceptor binding energy¹⁴ (0.046 eV) and the dielectric constant of InP (12.4) the acceptor Bohr radius is calculated to be only 1.2 nm. The unique-pair approximation is therefore valid.

According to the results presented in Appendix, the magnitude of the AS-DA resonance [Eqs. (A25)–(A28)] depends on the resonant change in the number of antisite-acceptor pairs in a particular charge state, while the magnitude of the AS-AS resonance [Eqs. (A20)–(A23)] depends primarily on the resonant change in the antisite spin polarization (the difference between the number of antisites in the $M = +\frac{1}{2}$ and $M = -\frac{1}{2}$

magnetic sublevels of the P_{In}^+ state). The relevant relaxation rate for the AS-DA resonance is thus the excited-state to ground-state recombination rate, while the relevant relaxation rate for the AS-AS resonance is determined either by the excited-to-ground recombination rate or by the spin-lattice relaxation rate, whichever is faster.

The amplitude of the ODMR signal, as a function of modulation frequency, begins to decrease at approximately the same frequency for both the AS-AS and AS-DA resonances [Figs. 6(a) and 6(b)], indicating that the relevant relaxation rate is approximately the same for both resonances. If the spin-lattice relaxation rate were faster than the excited-state recombination rate, then the AS-AS resonance would roll off at significantly higher frequency than the AS-DA resonance, contradicting the experimental result. There is a slight difference between the frequency dependences of the AS-AS and AS-DA resonances, but this is predicted by the model even when spin-lattice relaxation can be neglected, because of a difference in the behavior of the AS-AS and AS-DA resonances when the microwaves are switched on [compare Eq. (A22) with Eq. (A27)]. It thus appears that the spin-lattice relaxation rate of the antisite spin is much slower than the recombination rate, and has little effect on the kinetics of the ODMR.

The solid lines drawn through the data in Fig. 6 were obtained by fitting the data to the rate equation model with the value $R = 4 \times 10^4 \text{ s}^{-1}$ for the excited-state recombination rate. [For this fitting procedure, the results presented in Eqs. (A22)–(A23) and (A27)–(A28) were transformed from the time domain to the frequency domain in order to correspond to the data.] The model fits the in-phase data fairly well, but the peak of the quadrature response is broader than predicted, and also occurs at higher frequency than predicted for the AS-AS resonance [Fig. 6(a)]. These deviations from the model suggest that there is a distribution of recombination rates R for different antisite-acceptor pairs. This distribution most likely arises from a distribution of antisite-acceptor distances, which results in a more gradual frequency dependence than the one predicted by the single rate in the model.

The nature of the frequency dependence of the ODMR also depends on the quantum efficiency for radiative recombination of the antisite and acceptor η (i.e., the branching ratio between radiative and other recombination processes). For unity quantum efficiency, the AS-AS resonance would approach zero in the limit of low-frequency modulation, and would be largest at a frequency similar to the radiative recombination rate. [In the time domain, there would be a transient ODMR signal but no steady-state signal, as can be seen by setting $\eta = 1$ in Eqs. (A22)–(A23).] Experimentally, the AS-AS resonance is largest in the low-frequency limit and decreases monotonically with increasing frequency. The quantum efficiency must therefore be significantly less than unity. Numerical solutions of the rate equations in the frequency domain suggest that a monotonic decrease in the ODMR with increasing frequency is consistent with values of the quantum efficiency less than 0.4.

The experimentally observed magnitudes ($\Delta I/I_0$) of

the AS-DA and AS-AS resonances may be compared with the predictions of the rate-equation model. According to the model, the magnitude of the AS-AS resonance is $A\lambda(1-\eta)(\rho_e + \lambda\eta)$ [Eq. (A24)] and the magnitude of the AS-DA resonance is $F\lambda\eta(\rho_e + \lambda\eta)$ [Eq. (A29)]; also, the sign of the AS-AS resonance is positive (enhancing) and the sign of the AS-DA resonance is negative, in agreement with experiment. In these expressions, η is the quantum efficiency, λ is a parameter giving the spin dependence of the recombination rate, ρ_e is the initial spin polarization of the electron upon capture by the antisite, A is the fraction of the 0.8-eV PL that arises from antisites (other deep-level PL bands may overlap the antisite PL), and F is the fraction of acceptors that contribute to the shallow-donor to acceptor PL and are also paired with an antisite in the paramagnetic (P_{In}^+) state. As shown above, $\eta \leq 0.4$; the values of the parameters ρ_e and λ can be estimated as follows.

Because the initial photoexcitation energy is far above the bandgap, the electron spins should be thermalized in the conduction band before capture by the antisite defects; then $\rho_e = -\tanh(g_e\mu H/2kT)$ (the minus sign arises because, for positive g values, the spin-down state of the electron is lower in energy than the spin-up state). From the conduction-band electron g value of 1.22, the initial electron spin polarization is calculated to be $\rho_e = -0.11$ at $T=2$ K and $H=0.56$ T (the average of the magnetic fields at which the two hyperfine-split lines occur). The spin of the acceptor-bound hole should be completely thermalized; the parameter giving the spin dependence of the recombination rate between the $S=\frac{1}{2}$ electron and the thermalized $J=\frac{3}{2}$ hole is $\lambda = -5g_A\mu H/6kT$. (The spin-up state of the electron recombines more readily with the thermalized hole than the spin-down state, provided that the hole g value is positive; a minus sign is thus required to be consistent with the definition of λ at the beginning of the Appendix.) The shallow acceptor cannot be observed by spin resonance because of the orbital degeneracy of the $J=\frac{3}{2}$ state,¹⁵ making it difficult to determine the value of g_A . Hole g values in InP have been reported as 0.72 from Zeeman splitting of bound excitons¹⁶ in InP:Bi, 0.97 from magnetorefectance of free excitons,¹⁷ and 0.59 from Zeeman splitting of deep bound excitons¹⁸ in heat-treated InP; from the average of these values, we estimate $\lambda=0.12$.

From the values derived for η , ρ_e , and λ , the magnitude of the AS-AS resonance is calculated to be 1.3×10^{-2} (A), while the magnitude of the AS-DA resonance is calculated to be less than 7.6×10^{-3} (F); the experimental values (for the sum of the two hyperfine-split peaks at high microwave and optical power and low modulation frequency) are 1.2×10^{-3} and 1.6×10^{-3} , respectively. The values obtained for the remaining parameters are then $A=0.09$ and $F \geq 0.2$.

The large value obtained for F , the parameter that determines the relative magnitude of the AS-DA resonance, may imply an important result. If all acceptors are equally likely to contribute to the shallow-donor to acceptor PL, then F is just the ratio of the antisite concentration to the acceptor concentration. The P_{In}^+ con-

centration must then be greater than $2 \times 10^{15} \text{ cm}^{-3}$, because the acceptor concentration is 10^{16} cm^{-3} . The total concentration of antisites in all charge states is at least as large as the concentration of P_{In}^+ . Recalling that the maximum antisite concentration consistent with full compensation of the antisites by the Zn acceptors is $5 \times 10^{15} \text{ cm}^{-3}$, the antisite concentration appears to be determined to within a narrow range. The parameter F may, however, be significantly larger than the true antisite-acceptor ratio, if the acceptors that are paired with paramagnetic antisites are more likely to participate in shallow-donor to acceptor recombination than other acceptors. (Such a correlation might arise from several effects, for example selective excitation of acceptors paired with paramagnetic antisites, or a spatial correlation between the antisites and the shallow-donor impurities.) The lower limit on the antisite concentration is therefore still uncertain. In connection with this question, it is interesting to note that Deiri *et al.*⁸ previously suggested that the concentration of antisites in nonirradiated LEC-grown InP may be close to $5 \times 10^{15} \text{ cm}^{-3}$. (Deiri *et al.* reasoned that the apparent production of paramagnetic antisites at low electron irradiation levels may arise from a change in the charge state of preexisting antisites.)

It should be possible to describe the shallow-donor resonance of the shallow-donor to acceptor PL (Fig. 4) with rate equations analogous to those used for the antisite resonances. The simple rate-equation model would, however, predict an enhancing signal, just as for the AS-AS resonance [Eq. (A24)], while the shallow-donor resonance is actually observed to quench the shallow-donor to acceptor PL (Fig. 4). It may be that the rates for other transitions originating from the shallow-donor level, that compete with the shallow-donor to acceptor PL, are also spin dependent. (Spin dependence of the competing processes is arbitrarily excluded from the model presented in the Appendix in order to simplify the calculations.) Suppose that the shallow-donor resonance, while enhancing the rate of shallow-donor to acceptor recombination, also induces a proportionately greater increase in the rate of such a competing transition. The PL intensity would then decrease rather than increasing on resonance. One possible candidate for a competing spin-dependent transition is electron capture into the deep-donor level of a nearby antisite.

According to the model for the antisite ODMR, the magnitude of the ODMR signals [Eqs. (A24) and (A29)] is determined by products of the parameters λ and ρ_e , each of which represents the interaction of the antisite spin with a thermalized spin system (the acceptor-bound holes, or the electrons in the conduction band before capture by the antisites). As stated above, both λ and ρ_e are proportional to H/T . The magnitude of the ODMR should therefore vary as the square of the applied magnetic field or as the inverse square of the temperature. This prediction of the model can be tested by comparing the magnitudes of the two hyperfine-split ODMR peaks, which occur at significantly different values of the applied magnetic field. The ratio of the magnitudes of the high-

and low-field peaks is 1.47 for the AS-AS resonance, and 1.68 for the AS-DA resonance, as mentioned above, while the square of the ratio of the corresponding magnetic fields is 1.47. Results from a 24-GHz ODMR spectrometer provide further confirmation of the model; at the higher frequency, the ratio of the high- and low-field peaks is 1.21 (AS-AS resonance) while the square of the ratio of the fields is 1.27. (Note that the experimental test distinguishes between the proposed *indirect* thermalization mechanism and direct thermalization of the spins undergoing resonance: In the latter case, the relevant Boltzmann factor would be equal for two hyperfine-split resonances observed at the same resonant frequency, and the two peaks would be expected to have equal magnitudes.)

The dependence of the AS-DA resonance on photoexcitation intensity (Fig. 3) is the most difficult result to explain. The resonance first decreases with increasing intensity, then it increases, and, finally, appears to saturate at the highest intensities. It may be that holes are selectively captured by acceptors paired with paramagnetic (P_{in}^+) antisites at low intensities; then selective excitation becomes less important at intermediate intensities. At even higher intensities, the effect of the antisite resonance on the shallow-donor to acceptor recombination may increase again because the proportion of antisites in the paramagnetic state increases. Finally, at the highest intensities, all of the antisities may be converted to the paramagnetic state, causing the magnitude of the ODMR to saturate. It is perhaps possible to explain the intensity dependence of the AS-DA resonance by a combination of these effects. The monotonic decrease of the broad $g=2$ resonance (Figs. 2 and 3) with increasing intensity may perhaps be explained similarly, by the selective excitation at low intensity of acceptors paired to an unidentified deep defect.

V. CONCLUSION

The spin resonance of electrons bound to P_{in} antisites has been observed by PL ODMR in as-grown LEC InP:Zn with an acceptor concentration of 10^{16} cm^{-3} . The antisite resonance is observed as enhancing the antisite-to-acceptor PL at 0.8 eV and as quenching the competing shallow-donor to acceptor PL at 1.37 eV. The g value and hyperfine coupling constant are in good agreement with the values observed in electron-irradiated InP:Zn. The microwave power dependence confirms that the hyperfine-split resonance lines are further inhomogeneously broadened. The modulation frequency dependence shows that the spins of the antisite electrons are unthermalized (the spin-lattice relaxation time is long), the recombination is dominated by nonradiative processes, and the recombination rate of those pairs seen by ODMR is approximately $4 \times 10^4 \text{ s}^{-1}$. The relatively large magnitude of the quenching of the shallow-donor to acceptor PL by the antisite resonance suggests that the antisite concentration may be greater than $2 \times 10^{15} \text{ cm}^{-3}$. Two other ODMR signals are observed at 1.37 eV, both quenching: a broad resonance with $g=2.0$ which is observable only at low excitation intensity, and a narrow

resonance with $g=1.217$ which arises from shallow donors or possibly from conduction electrons.

ACKNOWLEDGEMENTS

We thank R. L. Henry of U. S. Naval Research Laboratory (NRL) for providing samples, W. D. Ohlsen of the University of Utah for assisting with these experiments, and N. D. Wilsey of NRL for useful discussions. This work was supported by the U. S. Office of Naval Research under Contract No. N00014-83-K-0535.

APPENDIX

Rate equations for the recombination of an $S = \frac{1}{2}$ electron bound to an antisite (or other deep donor) with a $J = \frac{3}{2}$ hole bound to an acceptor will be presented here and solved with reasonable approximations. The assumptions of the model follow.

(1) Each antisite is paired with one acceptor, in the sense that recombination between the antisite and paired acceptor is much more likely than recombination between the same antisite and any other acceptor. Because the donor may be occupied by a spin-up (\uparrow) or spin-down (\downarrow) electron or may be unoccupied (0), while the acceptor may be occupied by a hole (h) or unoccupied (0), the pair may exist in six different spin and charge states: ($\uparrow h$), ($\downarrow h$), (0h), ($\uparrow 0$), ($\downarrow 0$), and (00). (Different hole spin states are not distinguished, as explained in the next paragraph.)

(2) The hole spin is thermalized at a low temperature, and the electron-hole radiative recombination rate is therefore different for spin-up and spin-down electrons, because of the population imbalance among the various hole spin states. The radiative recombination rate is equal to $(1-\lambda)v_R$ for the ($\uparrow h$) state and to $(1+\lambda)v_R$ for the ($\downarrow h$) state. The rates for electron capture by the antisite, K_{\uparrow} and K_{\downarrow} , may also depend on the spin of the electron.

(3) The rates of non-spin-dependent recombination processes are v_{NR} for nonradiative recombination of the electron and hole, v_e for competing recombination of the electron (recombination external to the pair), and v_h for competing recombination of the hole. (The rate v_h includes, for example, recombination of the hole with an electron bound to a shallow donor.) The rate for hole capture by the acceptor K_h is also independent of electron spin.

(4) The rate for resonant transitions between the (\uparrow) and (\downarrow) electron spin states is equal to M ; this rate may be time dependent [$M = M(t)$] because the microwave field inducing the transitions is switched on and off.

Rate equations for the four states containing an electron may then be written

$$\begin{aligned} \frac{d}{dt} n_{\uparrow h} = & K_{\uparrow} n_{0h} + K_h n_{\uparrow 0} \\ & - [(1-\lambda)v_R + v_{NR} + v_e + v_h] n_{\uparrow h} \\ & - M(n_{\uparrow h} - n_{\downarrow h}), \end{aligned} \quad (A1)$$

$$\begin{aligned} \frac{d}{dt}n_{\downarrow h} &= K_{\downarrow}n_{0h} + K_h n_{\uparrow 0} \\ &\quad - [(1+\lambda)v_R + v_{NR} + v_e + v_h]n_{\downarrow h} \\ &\quad + M(n_{\uparrow h} - n_{\downarrow h}), \end{aligned} \quad (\text{A2})$$

$$\begin{aligned} \frac{d}{dt}n_{\uparrow 0} &= K_{\uparrow}n_{00} + v_h n_{\uparrow h} \\ &\quad - (K_h + v_e)n_{\uparrow 0} - M(n_{\uparrow 0} - n_{\downarrow 0}), \end{aligned} \quad (\text{A3})$$

$$\begin{aligned} \frac{d}{dt}n_{\downarrow 0} &= K_{\downarrow}n_{00} + v_h n_{\downarrow h} \\ &\quad - (K_h + v_e)n_{\downarrow 0} + M(n_{\uparrow 0} - n_{\downarrow 0}). \end{aligned} \quad (\text{A4})$$

To find an approximation that simplifies these equations, first add and subtract to obtain equations for the total electron density ($n_e = n_{\uparrow} + n_{\downarrow}$) and the difference between the spin-up and spin-down densities ($n_{\delta} = n_{\uparrow} - n_{\downarrow}$):

$$\begin{aligned} \frac{d}{dt}n_{eh} &= K_e n_{0h} + K_h n_{e0} + \lambda v_R n_{\delta h} \\ &\quad - (v_R + v_{NR} + v_e + v_h)n_{eh}, \end{aligned} \quad (\text{A5})$$

$$\frac{d}{dt}n_{e0} = K_e n_{00} + v_h n_{eh} - (K_h + v_e)n_{e0}, \quad (\text{A6})$$

$$\begin{aligned} \frac{d}{dt}n_{\delta h} &= K_{\delta} n_{0h} + \lambda v_R n_{eh} + K_h n_{\delta 0} \\ &\quad - (v_R + v_{NR} + v_e + v_h + 2M)n_{\delta h}, \end{aligned} \quad (\text{A7})$$

$$\frac{d}{dt}n_{\delta 0} = K_{\delta} n_{00} + v_h n_{\delta h} - (K_h + v_e + 2M)n_{\delta 0}. \quad (\text{A8})$$

Notice that the resonant transition rate (M) only appears in the equations for $n_{\delta h}$ and $n_{\delta 0}$, and acts to reduce these quantities (the spin polarizations).

Let us assume that the hole capture and release rates, K_h and v_h , are fast compared to the other rates in the problem. This should be a valid approximation because the hole is in a shallow acceptor level, while all the other rates (K_e , K_{δ} , v_R , λv_R , v_{NR} , and v_e) involve capture, release, or recombination of the electron in a deep level (the antisite). Then Eq. (A6) can be substituted into Eq. (A5) with the approximation $(d/dt)n_{e0} \sim v_h/K_h (d/dt)n_{eh}$ and Eq. (A8) can be substituted into Eq. (A7) with the approximation $(d/dt)n_{\delta 0} \sim v_h/K_h (d/dt)n_{\delta h}$. The resulting equations are

$$\frac{d}{dt}n_{eh} = K_e n_0^* + \lambda v_R^* n_{\delta h} - (v_R^* + v_{NR}^* + v_e)n_{eh}, \quad (\text{A9})$$

$$\frac{d}{dt}n_{\delta h} = K_{\delta} n_0^{**} + \lambda v_R^{**} n_{eh} - (v_R^{**} + v_{NR}^{**} + v_e + 2M)n_{\delta h}. \quad (\text{A10})$$

The newly defined parameters in the above equations are

$$n_0^* = \frac{K_h + v_e}{K_h + v_e + v_h} n_{0h} + \frac{K_h}{K_h + v_e + v_h} n_{00}, \quad (\text{A11})$$

$$\frac{v_R^*}{v_R} = \frac{v_{NR}^*}{v_{NR}} = \frac{K_h + v_e}{K_h + v_e + v_h}. \quad (\text{A12})$$

The parameters n_0^{**} , v_R^{**} , and v_{NR}^{**} are defined in almost the same way, except that v_e is replaced by $(v_e + 2M)$.

Suppose that the resonant transition rate M is either fast enough to satisfy the condition for saturation ($2M \gg v_R^{**} + v_{NR}^{**} + v_e$) or slow enough to be completely neglected ($M=0$). This should be the case experimentally when the microwave power is high and the microwave field is switched on and off with modulation amplitude of 100%. When $M=0$, the parameters with the single and double asterisks are equal ($v_R^{**} = v_R^*$). When the transition is saturated, Eq. (A10) has only the trivial solution $n_{\delta h}=0$. The difference between the parameters with the single and double asterisks can therefore be neglected when either of the above conditions is satisfied.

The main effect of the hole capture and release processes (K_h and v_h) is therefore simply to reduce the effective electron-hole recombination rate by the factor given in Eq. (A12). When the rate for competing recombination of the electron (v_e) is comparatively small, this factor is just the probability that the acceptor is in its occupied rather than its empty state.

Equations (A9) and (A10) can be further simplified by adding and subtracting again and by making the following definitions:

$$R = v_R^* + v_{NR}^* + v_e, \quad \eta = v_R^*/R, \quad n_0 = n_0^*. \quad (\text{A13})$$

The quantum efficiency η is the ratio of the radiative recombination rate to the total effective recombination rate. We obtain

$$\frac{d}{dt}n_{\uparrow h} = K_{\uparrow}n_0 - (1 - \lambda\eta)Rn_{\uparrow h} - M(n_{\uparrow h} - n_{\downarrow h}), \quad (\text{A14})$$

$$\frac{d}{dt}n_{\downarrow h} = K_{\downarrow}n_0 - (1 + \lambda\eta)Rn_{\downarrow h} + M(n_{\uparrow h} - n_{\downarrow h}). \quad (\text{A15})$$

The steady-state solutions when the spin-dependent recombination is weak ($\lambda\eta \ll 1$), and the resonant transition rate is $M=0$, are

$$N_{eh} = K_e n_0/R, \quad N_{\delta h} = (\rho_e + \lambda\eta)K_e n_0/R, \quad (\text{A16})$$

where the initial spin polarization is $\rho_e = K_{\delta}/K_e$.

Equations (A14) and (A15) can be solved easily if the following assumptions are valid: the resonant transition rate is switched between $M=0$ and a large value $M_{\text{sat}} \gg R/2$, and the frequency of switching is much smaller than R . The time-dependent solutions are

$$n_{\uparrow h}(t) = n_{\downarrow h}(t) = (N_{eh}/2) - (N_{\delta h}/2)\lambda\eta(1 - e^{-Rt}), \quad (\text{A17})$$

for $M = M_{\text{sat}}$ and

$$n_{\uparrow h}(t^*) = (N_{eh} + N_{\delta h})/2 - (N_{\delta h}/2)(1 + \lambda\eta)e^{-(1 - \lambda\eta)Rt^*}, \quad (\text{A18})$$

$$n_{\downarrow h}(t^*) = (N_{eh} - N_{\delta h})/2 + (N_{\delta h}/2)(1 - \lambda\eta)e^{-(1 + \lambda\eta)Rt^*}, \quad (\text{A19})$$

for $M=0$.

The initial times ($t=0$ or $t^*=0$) are the times when

the microwave field that induces resonant transitions is switched on or off; at $t=0$, the population of the ($\uparrow h$) state decreases suddenly by an amount equal to $N_{\delta h}$, and the population of the ($\downarrow h$) state increases by the same amount.

The time dependence of the PL intensity due to radiative recombination of the antisite and acceptor can now be determined from the equation

$$I_{\text{PL}}(t) = (1 - \lambda)\eta R n_{\uparrow h}(t) + (1 + \lambda)\eta R n_{\downarrow h}(t). \quad (\text{A20})$$

In the limit $\lambda\eta \ll 1$, the PL intensity off resonance ($M=0$) is

$$I_{\text{PL}}^0 = \eta R N_{eh} \quad (\text{A21})$$

and the change caused by the resonance is

$$\Delta I_{\text{PL}}(t) = \lambda\eta R N_{\delta h} [1 - \eta(1 - e^{-Rt})] \quad (\text{for } M = M_{\text{sat}}), \quad (\text{A22})$$

$$\Delta I_{\text{PL}}(t^*) = \lambda\eta R N_{\delta h} [1 - \eta(1 + Rt^*)] e^{-Rt^*} \quad (\text{for } M = 0). \quad (\text{A23})$$

If the quantum efficiency (η) approaches $\eta=1$ then transient changes in I_{PL} occur after the microwaves are switched (at $t=0$ or $t^*=0$), and decay at a rate R , but there is no steady-state change. If, on the other hand, $\eta \ll 1$, a steady-state change in I_{PL} occurs suddenly when the microwaves are switched on (at $t=0$); I_{PL} then decays to its initial value at rate R after the microwaves are switched off (at $t^*=0$).

The ratio of the steady-state change on resonance to the total PL intensity is

$$\Delta I_{\text{PL}}/I_{\text{PL}}^0 = (1 - \eta)\lambda(N_{\delta h}/N_{eh}) = (1 - \eta)\lambda(\rho_e + \lambda\eta). \quad (\text{A24})$$

The resonance is enhancing (I_{PL} increases when the resonance is switched on) if $\lambda(\rho_e + \lambda\eta) > 0$, or if ρ_e and λ have the same sign. As pointed out in the Discussion section, both ρ_e and λ are negative, according to the sign conventions we have chosen, provided that the electron and hole g values are both positive.

The PL intensity for a competing recombination process, such as shallow-donor to acceptor recombination, is

$$I_c(t) = v_c [n_{\uparrow h}(t) + n_{\downarrow h}(t) + n_{oh} + n_h^*], \quad (\text{A25})$$

where v_c is the radiative rate of the competing process, n_{oh} is the density of acceptors paired with unoccupied antisites, and n_h^* is the density of acceptors not paired with any antisite. (We assume that all acceptors contribute equally to the process.) The steady-state value of I_c is

$$I_c^0 = v_c N_{eh} / F, \quad F = N_{eh} / (N_{eh} + n_{oh} + n_h^*). \quad (\text{A26})$$

The change in the competing PL caused by the antisite resonance is

$$\Delta I_c(t) = -v_c \lambda \eta N_{\delta h} (1 - e^{-Rt}) \quad (\text{for } M = M_{\text{sat}}), \quad (\text{A27})$$

$$\Delta I_c(t^*) = -v_c \lambda \eta N_{\delta h} (1 + Rt^*) e^{-Rt^*} \quad (\text{for } M = 0). \quad (\text{A28})$$

There is a steady-state change in PL intensity on resonance; the change grows at rate R for $t > 0$, and decays at the same rate for $t^* > 0$. In contrast to the resonance detected directly on the antisite to acceptor PL [Eqs. (A20)–(A23)], no sudden change or transient overshoot occurs when the resonance is switched on. The competing PL is quenched ($\Delta I_c < 0$) under the same conditions that cause the direct PL to be enhanced ($\Delta_c > 0$). The ratio of the change caused by the resonance to the steady-state value of I_c is

$$\Delta I_c / I_c^0 = -F \lambda \eta (\rho_e + \lambda\eta). \quad (\text{A29})$$

As shown in the discussion section, the factors λ and ρ_e are each expected to vary with magnetic field and temperature as H/T . These factors occur in quadratic form in the expressions for the magnitude of the enhancing and quenching ODMR signals [Eqs. (A24) and (A29)]. Therefore, the magnitude of the ODMR is predicted to vary with magnetic field and temperature as $(H/T)^2$. Finally, the ratio of the fractional changes in PL intensity for the quenching and enhancing ODMR signals is found to be

$$(\Delta I_c / \Delta I_{\text{PL}}) (I_{\text{PL}}^0 / I_c^0) = -F \eta / (1 - \eta). \quad (\text{A30})$$

*Present address: National Bureau of Standards, Gaithersburg, MD 20899.

¹T. A. Kennedy and N. D. Wilsey, Appl. Phys. Lett. **44**, 1089 (1984).

²M. Deiri, A. Kana-ah, B. C. Cavenett, T. A. Kennedy, and N. D. Wilsey, J. Phys. C **17**, L793 (1984).

³A. Kana-ah, M. Deiri, B. C. Cavenett, N. D. Wilsey, and T. A. Kennedy, J. Phys. C **18**, L619 (1985).

⁴B. C. Cavenett, A. Kana-ah, M. Deiri, T. A. Kennedy, and N. D. Wilsey, J. Phys. C **18**, L473 (1985).

⁵T. A. Kennedy and N. D. Wilsey, J. Cryst. Growth **83**, 198 (1987).

⁶T. A. Kennedy, N. D. Wilsey, P. B. Klein, and R. L. Henry, Mater. Sci. Forum **10-12**, 271 (1986).

⁷D. Y. Jeon, H. P. Gislason, J. F. Donegan, and G. D. Watkins, Phys. Rev. B **36**, 1324 (1987).

⁸M. Deiri, A. Kana-ah, B. C. Cavenett, T. A. Kennedy, and N. D. Wilsey, Semicond. Sci. Technol. **3**, 706 (1988).

⁹B. C. Cavenett and E. J. Pakulis, Phys. Rev. B **32**, 8449 (1987).

¹⁰C. Weisbuch and C. Hermann, Solid State Commun. **16**, 659 (1975).

¹¹Yan Dawei, B. C. Cavenett, and M. S. Skolnick, J. Phys. C **16**, L647 (1983).

¹²D. Verity, J. J. Davies, and J. E. Nicholls, J. Phys. C **14**, (1981).

¹³D. J. Dunstan and J. J. Davies, J. Phys. C **12**, 2927 (1979).

¹⁴B. J. Skromme, G. E. Stillman, J. D. Oberstar, and S. S. Chan, J. Electron. Mater. **13**, 463 (1984).

¹⁵F. Mehran, T. N. Morgan, R. S. Title, and S. E. Blum, J. Magn. Res. **6**, 620 (1972).

¹⁶A. M. White, P. J. Dean, K. M. Fairhurst, W. Bardsley, and B. Day, J. Phys. C **7**, L35 (1974).

¹⁷D. Bimberg, K. Hess, N. O. Lipari, J. U. Fischbach, and M. Altarelli, Physica B + C **89B**, 139 (1977).

¹⁸K. R. Duncan, L. Eaves, A. Ramdane, W. B. Roys, M. S. Skolnick, and P. J. Dean, J. Phys. C **17**, 1233 (1984)